

dx.doi.org/10.17488/RMIB.43.1.3

E-LOCATION ID: 1216

A Chitosan-based Hydrogel with PLCL, ZnO NPs, and Oligoelements: A Promising Antibiotic Scaffold for Tissue Engineering

Hidrogel de Quitosano con PLCL, ZnO NPs y Oligoelementos: Un Andamio Antibacteriano Prometedor para Ingeniería de Tejidos

Yvain de los Ángeles Salinas Delgado¹ , Stephanie Soria Sánchez¹ , Gabriela Guadalupe Esquivel Barajas¹ ,
Eduardo Leos Quiñonez² , Luis Alberto Bretado Aragón¹ 

¹Universidad de La Ciénega del Estado de Michoacán de Ocampo

²Hospital Materno Infantil, Durango, Dgo.

ABSTRACT

Tissue engineering involves anchorage-dependent cells cultured on scaffolds, with growth factors added to facilitate cell proliferation. Its use in transplants implies the risk of bacterial infection. The current contribution describes the preparation and antibacterial evaluation of a chitosan-based hydrogel physically cross-linked with poly(L-lactic-co- ϵ -caprolactone) (PLCL) and enriched with zinc oxide nanoparticles (ZnO NPs) and trace elements (potassium and magnesium). The material was developed as a scaffold with built-in antibacterial properties. Chitosan and PLCL are biocompatible support materials applied in medicine for the repair and regeneration of damaged tissues, objectives promoted by ZnO NPs and the aforementioned trace elements. The ZnO NPs were elaborated by chemical coprecipitation. The materials were characterized by XRD, FT-IR, and SEM. Antibacterial testing was performed with strains of *Escherichia coli* and *Staphylococcus aureus* by the Kirby-Bauer method, in accordance with the NCCLS and CLSI guidelines. It was possible to obtain a homogeneous hydrogel with adequate morphology and distribution of elements. The hydrogel with 300 mM of Mg, K, and ZnO NP's showed antibacterial inhibition halos of 13 mm for *S. aureus* and 19 mm for *E. coli*. This innovative biomaterial with trace elements holds promise for tissue engineering by considering the challenge of bacterial infection.

KEYWORDS: Chitosan, PLCL, ZnO nanoparticles, Antibacterial, Tissue engineering

RESUMEN

La ingeniería de tejidos involucra el uso de células cultivadas en andamios con adiciones de factores de crecimiento para facilitar la proliferación celular. Su uso en trasplantes implica riesgo de infección bacteriana. La contribución actual describe la preparación y evaluación antibacteriana de un hidrogel a base de quitosano físicamente reticulado con poli (l-láctico-co- ϵ -caprolactona) (PLCL) enriquecido con nanopartículas de óxido de zinc (NP de ZnO) y oligoelementos (potasio y magnesio). El material se desarrolló como un andamio con propiedades antibacterianas. El quitosano y el PLCL son materiales de soporte biocompatibles aplicados en medicina para la reparación y regeneración de tejidos dañados, propiedades promovidas por las NP's de ZnO y los oligoelementos antes mencionados. Las NP de ZnO se elaboraron mediante coprecipitación química. Los materiales se caracterizaron por DRX, FT-IR y SEM. Las pruebas antibacterianas se realizaron con cepas de *Escherichia coli* y *Staphylococcus aureus* por el método de Kirby-Bauer de acuerdo con las guías NCCLS y CLSI. Se pudo obtener un hidrogel homogéneo con adecuada morfología y distribución de elementos. El hidrogel con 300 mM de NP ZnO y oligoelementos mostró halos de inhibición antibacteriana de 13 mm para *S. aureus* y 19 mm para *E. coli*. Este biomaterial innovador con oligoelementos es prometedor para la ingeniería de tejidos al considerar el desafío de la infección bacteriana.

PALABRAS CLAVE: Quitosano, PLCL, Nanopartículas ZnO, Antibacterial, Ingeniería de Tejidos

Corresponding author

TO: Luis Alberto Bretado Aragón

INSTITUTION: Universidad de La Ciénega del Estado de Michoacán de Ocampo

ADDRESS: Av. Universidad #3000, Col. Lomas de la Universidad, C. P. 59103, Sahuayo de Morelos, Michoacán, México

CORREO ELECTRÓNICO: labretado@ucemich.edu.mx

Received:

20 October 2021

Accepted:

24 January 2022

INTRODUCTION

Tissue engineering aims to establish, restore, or increase the function of tissues by means of the in vitro culturing of anchorage-dependent cells (either differentiated or undifferentiated) on scaffolds made of biomaterials. Growth factors are added to facilitate cell proliferation.

The in vitro tissues are then transplanted to a target organ [1] [2] with tissue injury. Such an injury is susceptible to infection by pathogenic microorganisms, which can lead to the loss or alteration of transplanted tissue, thus complicating tissue recovery and sometimes causing implant failure [1].

The biomaterials utilized in tissue engineering are biocompatible polymers, such as chitosan, that elicit robust cell proliferation [3]. The latter biopolymer is biocompatible, biodegradable, non-toxic, non-mutagenic, bioactive, cationic, antibacterial, and antifungal. It has been of great interest in developing drug-delivery scaffolds for tissue engineering and has been classified as “generally recognized as safe” (GRAS) by the US Food and Drug Administration (FDA) [4] [5]. Another material approved by the FDA to foster cell proliferation and adhesion is the poly(l-lactide-co-ε-caprolactone) (PLCL) polymer, due to its biocompatibility and mechanical properties [6].

Chitosan can be combined with certain trace elements essential for biological, physiological, and enzymatic processes. Consequently, zinc (Zn), potassium (K), and magnesium (Mg) [7] are added to improve certain functions, including protection against bacteria or fungi, bone regeneration, the synthesis of proteins, the absorption of Fe³⁺, the protection of tooth enamel, and the production of skin collagen [8] [9] [10]. ZnO nanoparticles (NPs), on the other hand, promote cell proliferation, growth, and differentiation. Additionally, their nanometric size affords high reactivity and thus favors an antibacterial effect [11].

During a surgical intervention for organ or tissue implantation, the main agents of infection are bacteria, which are able to generate septicemia, impetigo, cellulitis, skin abscesses, and even patient death [12]. The combination of chitosan, PLCL, ZnO NPs, and trace elements has an exciting future in tissue engineering. Apart from biocompatibility, this complex has the capacity for cell proliferation as well as inhibition of infection by nosocomial pathogens (e.g., *Staphylococcus aureus*, *Escherichia coli*, *Pseudomonas aeruginosa*, and *Serratia marcescens*) in surgical incisions and other medical conditions (e.g., diabetic foot and venous ulceration) [13].

The aim of the present study was to develop an HQT hydrogel with chitosan physically cross-linked to PLCL, with the addition of ZnO NPs and trace amounts of K and Mg. The ZnO NPs were obtained by chemical coprecipitation. The HQT hydrogel and its components were characterized with X-ray diffraction (XRD), Fourier transformed infrared spectroscopy (FT-IR), and scanning electron microscopy (SEM).

The antibacterial behavior of the HQT hydrogel was assessed with *S. aureus* ATCC® 25923 and *E. coli* ATCC® 25922 by means of the Kirby-Bauer method, in accordance with the international standards recommended by the Antimicrobial Susceptibility Testing Subcommittee of the National Committee for Clinical Laboratory Standards (NCCLS) [14] and the Clinical & Laboratory Standards Institute (CLSI) [15].

MATERIALS AND METHODS

a) Synthesis of ZnO NPs

Nanoparticles were synthesized by the coprecipitation method. A 4.46 mmol solution of zinc acetate (Sigma Aldrich, 99%) was prepared in 42 mL of methanol (Meyer, 99%) by magnetic stirring at 600 rpm and 60 °C. A 7.22 mmol solution of

potassium hydroxide (KOH) (Sigma Aldrich, 99%) was prepared in 23 ml of methanol as a precipitating agent. The resulting mixture was added dropwise to the zinc solution, followed by stirring at 600 rpm and 60 °C for 3 h. The white precipitate was washed with acetone and water, and then heated at 60 °C in an oven for 12 h.

b) Characterization of ZnO NPs and the hydrogel by XRD, FT-IR, and SEM

The ZnO nanoparticles were characterized by X-ray diffraction with a Bruker D8 Advance diffractometer, with a Cu α source at 30 mA and 30 kV and a scanning speed of 1.2° steps/min (in the range of 10-80 2 θ degrees). The size of the crystallites was determined by means of the Scherrer equation. FT-IR analysis of the samples was carried out in a PerkinElmer Frontier FT-IR spectrometer at a wavelength of 4000 to 400 cm⁻¹. Scanning electron microscope analysis of the ZnO NPs and the hydrogel were performed on a JEOL JSM 6100 SEM at 20 kV, after coating the materials with gold for 40 s.

c) Preparation of the HQT hydrogel

The concentration of the elements contained in the hydrogel was previously defined by considering the bactericidal effect. A 2% (w/v) solution of chitosan (Sigma Aldrich, at a medium molecular weight and 85% deacetylated) was prepared in 1 M glacial acetic acid (Sigma Aldrich) and stirred at 600 rpm until dissolved. Subsequently, ZnO NPs, K, and Mg were each adjusted to a concentration of 300 mM. KCl₂ and MgCl₂ (Sigma Aldrich, 99%) were the precursors of K and Mg. PLCL (Sigma Aldrich) at 0.2 % (w/v) was added and the mixture was stirred at 600 rpm for 12 h. The hydrogel was heated in an oven at 40 °C for 48 h to promote the crosslinking reaction.

d) Antibacterial evaluation

The antibacterial activity of the HQT hydrogel was assessed with *E. coli* ATCC® 25922 and *S. aureus* ATCC® 25923 by means of the disk diffusion (Kirby Bauer) method in BD Mueller Hinton agar, following the CLSI guidelines. The turbidity of the bacterial suspension was adjusted to a 0.5 McFarland standard (1.5x10⁸ CFU/ml) and then incubated for 24 h at 37 °C. Inhibition was shown as a clear circular zone and the diameter was measured in mm, indicating bacterial susceptibility to the sample under study. BD BBL Sensi-Disc™ antimicrobial sensitivity test discs (Becton Dickinson) of amoxicillin/clavulanic acid (30 µg) were used as the positive control for inhibition.

RESULTS AND DISCUSSION

a) Characterization by XRD, FT-IR, and SEM

ZnO NPs were characterized by SEM and XRD (Figure 1). The micrograph (Figure 1a) of the surface of the ZnO powder, viewed at 5000X, displays agglomerates of particles with irregular morphology. By analyzing the energy-dispersive X-ray spectroscopy (EDS, Fig. 1b) and elemental mapping (Figs. 1c, d), peaks corresponding to oxygen and zinc were identified on the surface of the material. Hence, the synthesis was successful. Moreover, the product had no contaminants. The diffractogram (Fig. 1e) exhibits peaks corresponding to the zincite phase (according to PDF #04-003-2106) in space group P63mc, with lattice parameters $a=3.25010\text{\AA}$ and $c=5.20710\text{\AA}$. Characteristic reflections were observed in the (100), (002), (101), (102), (110), (103), (112), and (202) lattice planes, similar to those found by Purwaningsih *et al.* 2016 [16]. The size of the crystallites was 30 nm, calculated with the Scherrer equation. No secondary phases were formed during synthesis.

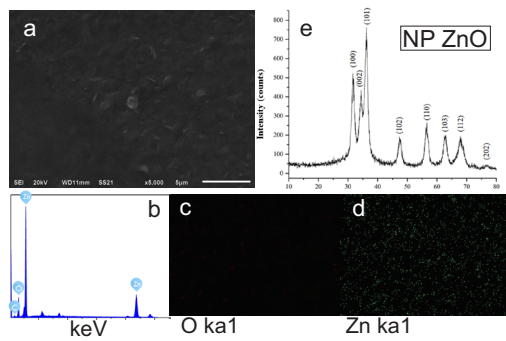


FIGURE 1. Characterization of ZnO NPs:

a) Surface micrograph at 5000X; b) EDS spectrum; elemental mapping for c) oxygen and d) zinc; and e) the XRD pattern.

The hydrogel was morphologically characterized by SEM before and after adding the trace elements and the ZnO NPs (Figure 2). Before adding anything, chitosan displayed a smooth texture and large pores distributed all along the surface (Figure 2.1 a). The porosity of the hydrogel is a critical factor since it allows for the anchoring of cells and the loading of different drugs, elements, or biologically relevant substances. After adding the trace elements and the ZnO NPs (Figure 2.2 a), the surface had a distinct appearance. The particles were coated by a chitosan matrix. By comparing the results of EDS and elemental mapping (Figs. 2.1 b and 2.2 b), it was possible to identify carbon (C), nitrogen (N), and oxygen (O) (Figs. 2.1 c, d and e) in the hydrogel without trace elements. With the addition of these elements, a good distribution of Mg, K, and Zn existed on the surface of the hydrogel (Figs. 2.2 c, d and e). A chlorine (Cl) peak was also found for the inadequately washed hydrogels.

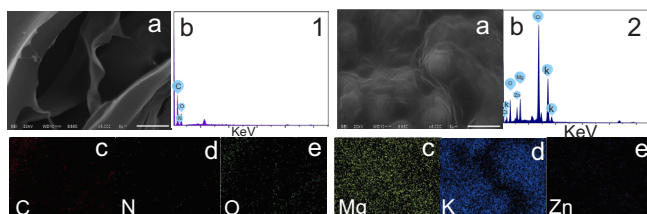


FIGURE 2. SEM spectra of the hydrogel. 1) Before adding trace elements, and 2) after adding them. Micrographs (a), EDS spectra (b), and elemental mapping (c, d, e, and f).

Correct washing eliminates the Cl residues derived from the precursors of the trace elements (KCl_2 and $MgCl_2$). During the microscopy analysis, no damaged or detached zones were detected on the hydrogel, which indicates that the physical crosslinking with PLCL was optimal.

The FT-IR spectra are shown for trace elements, PLCL, and the hydrogel (Figure 3). All samples were dissolved in 1 M acetic acid. The vibrational bands of ~ 3398 - 3300 cm^{-1} and 1637 cm^{-1} in spectra 1, 2, and 3 can be attributed to the OH group in the solvent [17]. The spectrum of chitosan (Figure 3.4) exhibits a band at ~ 3323 cm^{-1} for the OH/NH groups, at ~ 1644 cm^{-1} for C-N, at ~ 1392 cm^{-1} for C=O, and at ~ 1288 cm^{-1} for C-O-C (corresponding to amine 1), C-H vibrations, and C-C and C-O stretching (corresponding to amine 3), respectively [18] [19].

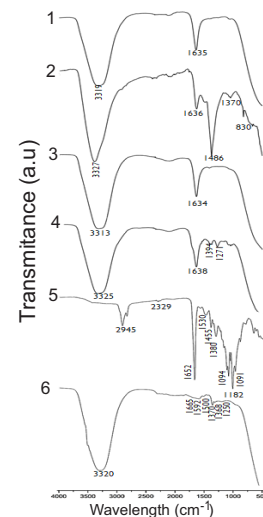


FIGURE 3. FT-IR spectra for the Mg precursor (1), the K precursor (2), ZnO NPs (3), chitosan (4), PLCL (5), and the HQT hydrogel (6).

The main contributions of PLCL are seen in Figure 3.5. The band at ~ 2980 cm^{-1} is assigned to alkyl stretching, at ~ 1750 cm^{-1} to carbonyl stretching, at ~ 1700 cm^{-1} to carbonyl ester stretching, and at ~ 1450 cm^{-1} to CH_2 bending. The bands at ~ 1380 cm^{-1} were ascribed to C=O, at ~ 1189 cm^{-1} and ~ 1182 cm^{-1} to C-O-O and asymmetric CH_2 , and at ~ 1091 cm^{-1} to the stretching vibrations of C-O [20].

The FT-IR absorption bands of the HQT hydrogel (with all its components) are shown in Figure 3.6, observing a clear difference in the interaction of the functional groups. The bands at $\sim 3300\text{ cm}^{-1}$ were designated as the NH_2 and OH groups, at $\sim 1750\text{ cm}^{-1}$ as the stretching of the carbonyl groups in PLCL, at $\sim 1600\text{ cm}^{-1}$ as the CH_2 and CH_3 groups, and at $\sim 1250\text{ cm}^{-1}$ as a stretching of the C-O-C present in chitosan. Finally, the band at $\sim 1420\text{ cm}^{-1}$ may be due to the chitosan CH_2 groups or PLCL-COO- groups [18] [19] [20].

b) Antibacterial activity

The antibacterial effect of the HQT hydrogel was evaluated with *E. coli* and *S. aureus*. The inhibition zones were more evident for *S. aureus* (25 mm for chitosan and 14 mm for ZnO NPs) than *E. coli* (14 mm for chitosan and 7 mm for ZnO NPs) (Figure 4). This result is attributed to the innate antimicrobial activity of chitosan and the oxidative stress caused by ZnO nanoparticles. Regarding the latter, reactive oxygen species (ROS) interact with the cell wall of bacteria and destroy the intracellular content, damaging proteins and lipids. Hence, positively charged nanoparticles bind to the negatively charged bacterial membrane, fomenting its disintegration or rupture [21]. Additionally, the size of ZnO NPs is effective against Gram-positive and Gram-negative bacteria because of the large surface area available to interact with the bacterial wall [22].

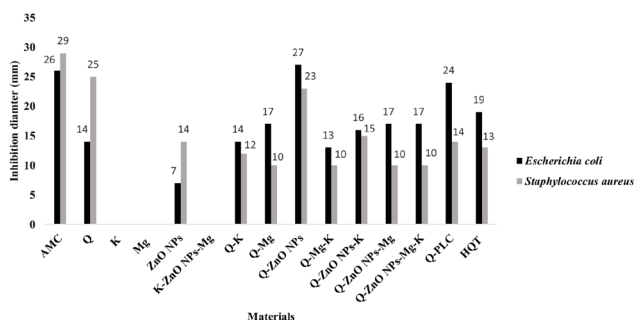


FIGURE 4. Inhibition zones (in mm) of *E. coli* and *S. aureus* exposed to the biomaterials herein tested.

For the biomaterials with trace elements, the inhibition of *E. coli* was more significant than that of *S. aureus*. The content of K and Mg affect the antibacterial activity of ZnO NPs, as can be appreciated by the lack of inhibition of both microorganisms. Concerning *E. coli*, the inhibition diameters resulting from K combined with Q (Q-K) materials were very similar to those found with chitosan alone (14 mm). The antibacterial effect of Q-K materials on *S. aureus* was reduced by about 50% (to 12 mm) (Figure 4).

K is required by microorganisms for the metabolism of carbohydrates, the activation of some enzymes, and bacterial osmoregulation [23]. Therefore, it is herein inferred that K was mainly used as a nutrient by the bacteria rather than a growth inhibitor. For *E. coli*, the inhibition diameter was greater with Q-Mg (17 mm) than chitosan alone (14 mm). Thus, Mg increased the antibacterial potential of chitosan. Mg and K did not show any antibacterial activity separately. They participate in vital functions as nutrients [23], which was probably their primary role. Q-PLCL generates a good antibacterial effect on *E. coli*, with an inhibition diameter of 24 mm. Finally, the HQT hydrogel significantly inhibited *S. aureus* (13mm) and *E. coli* (19mm), the latter being more susceptible.

The values of the inhibition diameters are observed in Figures 4 and 5. In both, the importance of the inhibitory activity of chitosan is evidenced by its greater inhibition diameter for all combinations. The concentration of 300 mM of the trace elements promoted bacterial inhibition in some of the materials. This concentration was determined in a previous study employing the same bacteria. The tests were conducted by means of the Kirby-Bauer method, exposing each bacteria to the biomaterials presently evaluated.

E. coli and *S. aureus* are common pathogens responsible for tissue infection. Due to the structural and chemical differences of their cell walls, it was relevant

to evaluate the inhibitory effect of the present biomaterials on both species ^[13]. According to the literature, chitosan, PLCL and ZnO NPs are non-toxic materials and have been used in various biomedical applications. The current results indicate that combining biomaterials on a chitosan hydrogel scaffold holds promise for combatting tissue infection caused by bacteria. Future research is necessary to examine the cytotoxicity of the hydrogel.

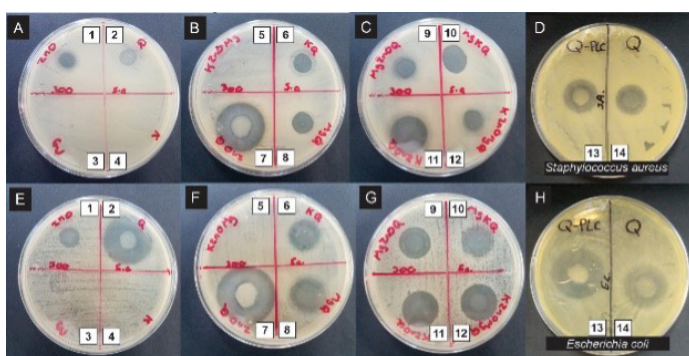


FIGURE 5. Results of the Kirby-Bauer method to examine the antibacterial effect of the HQT hydrogel with distinct combinations of trace elements and ZnO NPs. *S. aureus*: A, B, C, and D; *E. coli*: E, F, G, and H. 1) ZnO NPs; 2) Q; 3) Mg; 4) K; 5) K-ZnO NPs-Mg; 6) Q-K; 7) Q-ZnO NPs; 8) Q-Mg; 9) Q-ZnO NPs-Mg; 10) Q-Mg-K; 11) Q-ZnO NPs-K; 12) HQT; 13) Q-PLCL; and 14) Q.

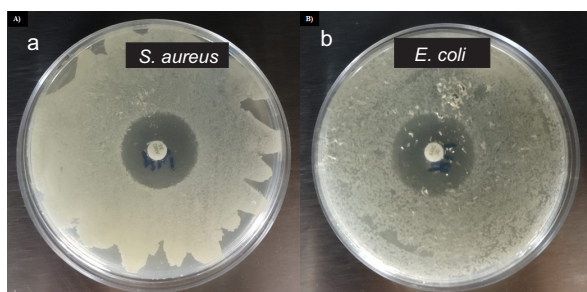


FIGURE 6. Inhibition produced by the antibiotic disc (the positive control), containing amoxicillin/clavulanic acid (30 µg). A) *S. aureus*; B) *E. coli*.

CONCLUSIONS

Zinc oxide nanoparticles of 30 nm were obtained in the zincite phase. It was possible to elaborate an adequately homogenized chitosan-based hydrogel physically cross-linked with PLCL and enriched with ZnO NPs as well as trace amounts of Mg and K. In vitro testing showed that this hydrogel has antibacterial activity. Since these biomaterials are organic, FDA-approved, and biocompatible with different biological systems, the resulting hydrogel represents a potentially useful antibiotic scaffold for tissue engineering.

ETHICAL STATEMENT

The test and experiments realized with bacteria are conducted under strict protocols and procedures approved internationally; before, during and after the test were carried out.

AUTHOR CONTRIBUTIONS

Y.A.S.D. designed the original project, carried out analyses like spectroscopic characterization, bacterial tests, contributed to the writing of the several stages of the manuscript, attended editorial reviews and provided materials and reagents. S.S.S. synthesized materials and carried out bacterial assays and spectroscopic characterization, participated in writing the original manuscript. G.G.E.B. participated in doing research and characterization of materials and in writing the original manuscript. E.L.Q. assisted in the analysis of the bacterial testing results and participated in writing the original manuscript. L.A.B.A. designed the original project, supervised, and validated the synthesis and characterization of the hydrogel, carried out several analyses and contributed to the writing of the several stages of the manuscript and attended editorial reviews and provided materials and reagents. All authors approved the final version of the manuscript.

REFERENCES

- [1] Serrato Ochoa D, Nieto Aguilar R, Aguilera Méndez A. Ingeniería de tejidos. Una nueva disciplina en medicina regenerativa. *Investig Cienc* [Internet]. 2015;23(64):61-69. Available from: <https://www.redalyc.org/articulo.oa?id=67441039009>
- [2] Abdulghani S, Mitchell GR. Biomaterials for In Situ Tissue Regeneration: A Review. *Biomolecules* [Internet]. 2019;9(11):750. Available from: <https://doi.org/10.3390/biom9110750>
- [3] Gough JE, Scotchford CA, Downes S. Cytotoxicity of glutaraldehyde crosslinked collagen/poly(vinyl alcohol) films is by the mechanism of apoptosis. *J Biomed Mater Res* [Internet]. 2002;61(1):121-130. Available from: <https://doi.org/10.1002/jbm.10145>
- [4] Patrulea V, Ostafe V, Borchard G, Jordan O. Chitosan as a starting material for wound healing applications. *Eur J Pharm Biopharm* [Internet]. 2015;97(Part B):417-26. Available from: <https://doi.org/10.1016/j.ejpb.2015.08.004>
- [5] Ortega Cardona CE, Aparicio Fernández X. Quitosano: una alternativa sustentable para el empaque de alimentos. *RDU* [Internet]. 2020; 21(5):1-9. Available from: <https://doi.org/10.22201/cuaieed.16076079e.2020.21.5.4>
- [6] He Y, Liu W, Guan L, Chen J, et al. A 3D-Printed PLCL Scaffold Coated with Collagen Type I and Its Biocompatibility. *BioMed Res Int* [Internet]. 2018;2018:5147156. Available from: <https://doi.org/10.1155/2018/5147156>
- [7] Spears JW, Engle TE. Feed Ingredients: Feed Supplements: Microminerals. *Encyclopedia of Dairy Sciences* [Internet]. 2011. 378-383. Available from: <https://doi.org/10.1016/B978-0-08-100596-5.00760-5>
- [8] Bhattacharya PT, Misra SR, Hussain M. Nutritional Aspects of Essential Trace Elements in Oral Health and Disease: An Extensive Review. *Scientifica* [Internet]. 2016;2016:5464373. Available from: <https://doi.org/10.1155/2016/5464373>
- [9] Silva CS, Moutinho CG, Vinha AF, Matos CM. Trace Minerals in Human Health: Iron, Zinc, Copper, Manganese and Fluorine. *Int J Sci Res Methodol* [Internet]. 2019;13(3):57-80. Available from: https://bdigital.ufp.pt/bitstream/10284/8105/1/5.Customer-IJSRM_HUMAN-13_8-19-27-08-2019%20%282%29.pdf
- [10] Gao C, Peng S, Feng P, Shuai C. Bone biomaterials and interactions with stem cells. *Bone Res* [Internet]. 2017;5:17059. Available from: <https://doi.org/10.1038/boneres.2017.59>
- [11] Laurenti M, Cauda V. ZnO Nanostructures for Tissue Engineering Applications. *Nanomaterials* [Internet]. 2017;7(11):374. Available from: <https://doi.org/10.3390/nano7110374>
- [12] Ribeiro M, Monteiro FJ, Ferraz MP. Infection of orthopedic implants with emphasis on bacterial adhesion process and techniques used in studying bacterial-material interactions. *Biomater* [Internet]. 2012;2(4):176-194. Available from: <https://dx.doi.org/10.4161%2Fbiom.22905>
- [13] Blanes JI, Clará A, Lozano F, Alcalá D, et al. Consensus document on the treatment of diabetic foot infections. *Angiología* [Internet]. 2012;64(1):31-59. Available from: <https://doi.org/10.1016/j.angio.2011.11.001>
- [14] National Committee for Clinical Laboratory Standards. Methods for determining bactericidal activity of antimicrobial agents: approved guideline [Internet]. Wayne, PA: National Committee for Clinical Laboratory Standards; 1999. Available from: https://webstore.ansi.org/preview-pages/CLSI/preview_M26-A.pdf
- [15] Clinical and Laboratory Standards Institute. Performance Standards for Antimicrobial Susceptibility Testing. CLSI supplement M100 [Internet]. Wayne, PA: Clinical and Laboratory Standards Institute; 2017. Available from: <https://file.qums.ac.ir/repository/mmrc/clsi%202017.pdf>
- [16] Purwaningsih SY, Pratapa S, Triwikantoro, and Darminto. Nano-sized ZnO powders prepared by co-precipitation method with various pH. *AIP Conf Proc* [Internet]. 2016;1725:020063.1-020063.6. Available from: <https://doi.org/10.1063/1.4945517>
- [17] Colomer MT. Straightforward synthesis of Ti-doped YSZ gels by chemical modification of the precursors alkoxides. *J Sol-Gel Sci Technol* [Internet]. 2013;67:135-144. Available from: <https://doi.org/10.1007/s10971-013-3059-9>
- [18] Maldonado Lara K, Luna Bárcenas G, Luna Hernández E, Padilla Vaca, et al. Preparation and characterization of Copper Chitosan Nanocomposites with Antibacterial Activity for Applications in Tissue Engineering. *Rev Mex Ing Biomed* [Internet]. 2017;38(1):306-313. Available from: <https://dx.doi.org/10.17488/RMIB.38.1.26>
- [19] Varma R, Vasudevan S. Extraction, Characterization, and Antimicrobial Activity of Chitosan from Horse Mussel *Modiolus modiolus*. *ACS Omega* [Internet]. 2020;5(32):20224-20230. Available from: <https://doi.org/10.1021/acsomega.0c01903>
- [20] Garkhal K, Verma S, Jonnalagadda S, Kumar N. Fast degradable poly(L-lactide-co-e-caprolactone) microspheres for tissue engineering: Synthesis, characterization, and degradation behavior. *J Polym Sci A: Polym Chem* [Internet]. 2007;45(13):2755-2764. Available from: <https://doi.org/10.1002/pola.22031>
- [21] Zavaleta EG, Saldaña JJ, Jáuregui RSR, Pacherrez GMD, et al. Antibacterial effect of ZnO nanoparticles on *Staphylococcus aureus* and *Salmonella typhi*. *Arnaldoa* [Internet]. 2019;26(1):421-432. Available from: <http://dx.doi.org/10.22497/arnaldoa.261.26122>
- [22] Yamamoto O. Influence of particle size on the antibacterial activity of zinc oxide. *Int J Inorg Mater* [Internet]. 2001;3(7):643-646. Available from: [https://doi.org/10.1016/S1466-6049\(01\)00197-0](https://doi.org/10.1016/S1466-6049(01)00197-0)
- [23] Stautz J, Hellmich Y, Fuss MF, Silberberg JM, et al. Molecular Mechanisms for Bacterial Potassium Homeostasis. *J Mol Biol* [Internet]. 2021;433(16):166968. Available from: <https://doi.org/10.1016/j.jmb.2021.166968>